Title

A Histidine Cluster in the Cytoplasmic Domain of the Na-H Exchanger NHE1 Confers pH-sensitive Phospholipid Binding and Regulates Transporter Activity*

Permalink

https://escholarship.org/uc/item/3sw6f0hf

Journal

Journal of Biological Chemistry, 291(46)

ISSN

0021-9258

Authors

Webb, Bradley A
White, Katharine A
Grillo-Hill, Bree K
et al.

Publication Date

2016-11-01

DOI

10.1074/jbc.m116.736215

Peer reviewed

A Histidine Cluster in the Cytoplasmic Domain of the Na-H Exchanger NHE1 Confers pH-sensitive Phospholipid Binding and Regulates Transporter Activity

Bradley A. Webb[1], Katharine A. White[1], Bree K. Grillo-Hill[1,3], André Schönichen[1,4], Changhoon Choi[2], and Diane L. Barber[1]

[1] Department of Cell and Tissue Biology, University of California, San Francisco
[2] Department of Radiation Oncology, Samsung Medical Center, Seoul South Korea

Current address
[3]Department of Biological Sciences, San Jose State University, San Jose, CA
[4]Amgen Inc., South San Francisco, CA

Running title – pH-Sensitive Phospholipid Binding Regulates NHE1 Activity

To whom correspondence should be addressed: Prof Diane L. Barber, Department of Cell and Tissue Biology, University of California, San Francisco, 513 Parnassus Ave, HSW618, Box 0512, San Francisco, California, 94143, FAX: 415-502-7338; Email: diane.barber@ucsf.edu

ABSTRACT

The Na-H exchanger NHE1 contributes to intracellular pH (pHi) homeostasis in normal cells and the constitutively increased pHi in cancer. NHE1 activity is allosterically regulated by intracellular protons, with greater activity at lower pHi. However, the molecular mechanism for pH-dependent NHE1 activity remains incompletely resolved. We report that an evolutionarily conserved cluster of histidine residues located in the C-terminal cytoplasmic domain between two phosphatidylinositol 4,5-bisphosphate-binding sites ($PI(4,5)P_2$) of NHE1 confers pH-dependent $PI(4,5)P_2$-binding and regulates NHE1 activity. A GST-fusion of the wild-type C-terminal cytoplasmic domain of NHE1 showed increased maximum $PI(4,5)P_2$ binding at pH 7.0 compared to pH 7.5. However, pH-sensitive binding is abolished by substitutions of the His-rich cluster to arginine (RxxR3) or alanine (AxxA3), mimicking protonated and neutral histidine residues respectively, and the RxxR3 mutant had significantly greater $PI(4,5)P_2$ binding than AxxA3. When expressed in cells, NHE1 activity and pHi were significantly increased with NHE1-RxxR3 and decreased with NHE1-AxxA3 compared with wild-type NHE1. Additionally, fibroblasts expressing NHE1-RxxR3 had significantly more contractile actin filaments and focal adhesions compared with fibroblasts expressing wild-type NHE1, consistent with increased pHi enabling cytoskeletal remodeling. These data identify a molecular mechanism for pH-sensitive $PI(4,5)P_2$ binding regulating NHE1 activity and suggest that the evolutionarily conserved cluster of four histidines in the proximal cytoplasmic domain of NHE1 may constitute a proton modifier site. Moreover, a constitutively activated NHE1-RxxR3 mutant is a new tool that will be useful for studying how increased pHi contributes to cell behaviors, most notably the biology of cancer cells.

Intracellular pH (pHi) homeostasis is generally maintained near neutral to compensate for metabolic changes and environmental stresses (1). However, dysregulated pHi is seen in a number of diseases. Most cancers have constitutively increased pHi of ~ 0.4 units, which enables proliferation and metastasis (2-4). Conversely, neurodegenerative disorders, including Parkinson's and Alzheimer's diseases, are associated with constitutively decreased pHi, which is predicted to enable tau and β-amyloid aggregation as well as cell death (5, 6). Finely tuned pHi homeostasis is maintained by dynamic changes in ion transporter activity that is sensitive to intracellular proton concentrations. However, the molecular mechanisms that mediate pH sensing by ion transporters remain poorly understood.

The ubiquitously expressed Na-H exchanger isoform NHE1 contributes to maintaining pHi homeostasis by generating an electroneutral influx of extracellular Na^+ and efflux of intracellular H^+ at the plasma membrane. To maintain pHi homeostatsis, NHE1 activity increases with acidic pHi and becomes nearly quiescent at neutral pHi. However, NHE1 activity can be increased at neutral pHi in response to growth factor signaling or activated oncogenes by direct phosphorylation of serine residues in the distal C-terminal cytoplasmic domain by kinases such as p90RSK (7), Akt (8), the Rho kinase ROCK (9), and the Nck-interacting kinase NIK (also called MAP4K4) (10). In response to oncogenes, phosphorylation-dependent increases in NHE1 activity override pH-dependent regulation, resulting in the higher pHi in cancer (3). In contrast to how NHE1 activity is regulated by kinases, how it is regulated by acidic pHi remains unclear. More than 30 years ago Aronson and colleagues first proposed a pH-dependent proton modifier site in the C-terminal cytoplasmic domain (11), but to date this site remains incompletely defined.

Since the first prediction of a proton modifier site regulating NHE1 activity (11), binding to the negatively charged plasma membrane phospholipid phosphatidylinositol 4,5-bisphosphate PI(4,5)P2 emerged as a mechanism for increasing activity of different classes of ion transport proteins (12). The Grinstein and Orlowski groups showed the importance of PI(4,5)P2 binding for increased activity for NHE1 that is dependent on two positively charged regions in the membrane-proximal C-terminal cytoplasmic domain (^{509}KKKQETKR^{515} and ^{552}RFNKKYVKK^{560} for human NHE1) (13) and subsequently identified electrostatic interactions between PI(4,5)P2 and homologous basic residues in the NHE3 isoform (14). Schelling and colleagues showed that electrostatic interactions between NHE1 and PI(4,5)P2 are dependent on arginine and lysine residues in these two positively charged regions in the C-terminal cytoplasmic domain of NHE1 and also that PI(4,5)P2 binding is pH-dependent, with higher binding affinity at lower pH (15). However, arginine and lysine with pKa's of 12 and 10.5 in solution, respectively, likely do not titrate with physiological changes in pH to confer pH-dependent binding to PI(4,5)P2 .

We report that a cluster of histidine (His) residues between the two positively charged regions in the C-terminal cytoplasmic domain (^{540}HYGHHH^{545} for human NHE1) regulate pH-dependent PI(4,5)P2 binding and transporter activity. We generated protonated and neutral mimetics by substituting these histidine residues with arginine (NHE1-RxxR3) and alanine (NHE1-AxxA3), respectively, which abolished pH-sensitive PI(4,5)P2 binding *in vitro*. When expressed in fibroblasts, NHE1-RxxR3 was constitutively active, with

2

greater quiescent activity than wild-type NHE1, and conferred higher quiescent pHi as well as increased abundance of contractile actin filaments and cell-substrate adhesions. In contrast, NHE1-AxxA3 had lower quiescent activity than wild-type NHE1, and unlike wild-type NHE1, its activity did not increase in response to platelet-derived growth factor. Our findings show that an evolutionarily conserved cluster of four His residues in NHE1 regulate transporter activity and suggest that this cluster may constitute an NHE1 proton modifier site first proposed more than 30 years ago.

RESULTS

Cluster of histidine residues in proximal C-terminal cytoplasmic domain confer pH-dependent $PI(4,5)P_2$ binding—Based on previous findings that the proximal C-terminus of NHE1 has pHi-dependent $PI(4,5)P_2$ binding (15), we reasoned that this may be mediated by histidine residues, which can titrate within the physiological pH range and function as a pH sensor site (16). We identified a series of histidine residues located between the arginine/lysine-rich regions that bind $PI(4,5)P_2$ (Fig. 1A), which are invariant in vertebrate NHE1 orthologs (Fig. 1B). Histidines flanked by arginine/lysine-rich regions in the proximal C-terminus are also conserved in other plasma membrane NHE isoforms, although the number of histidine residues varies with isoforms having between one and four (Fig. 1C).

We used an ELISA assay to measure pH-dependent $PI(4,5)P_2$ binding by GST-fusion proteins of the C-terminal cytoplasmic domain of human NHE1 (amino acids 503-815; Fig. 2). The assay used $PI(4,5)P_2$-coated multiwell plates and showed that wild-type NHE1$^{503-815}$ (NHE1-WT) had decreased binding at pH 7.5 compared with 7.0, as previously described (15). Maximal binding (B_{max}) was $0.87 \pm$

0.04 arbitrary units (a.u.) at pH 7.5 and 1.0 ± 0.04 a.u. at pH 7.0 ($p<0.05$; mean $\pm$ SD; Fig. 2A and Table 1). Additionally, binding affinity was lower at pH 7.5 compared with pH 7.0, with dissociation constants (k_d) of 65 ± 10 nM and 38 ± 6 nM, respectively ($p<0.05$; Table 1).

We next asked whether the cluster of histidines between the arginine/lysine-rich regions (Fig. 1B) is important for pH-dependent $PI(4,5)P_2$ binding. We generated mutant GST-fusions of the C-terminal cytoplasmic domain by substituting the four histidines in the cluster with arginines for a protonated mimetic (NHE1-RxxR3) or with alanines for a neutral mimetic (NHE1-AxxA3). Although both mutants bound PI(4,5)P2, pH-dependent binding was abolished, with no significant differences in B_{max} or k_d for each mutant at pH 7.5 compared with pH 7.0 (Fig. 2B,C; Table 1). However, B_{max} for RxxR3 was significantly greater than AxxA3 at pH 7.5 and pH 7.0 ($p<0.05$), and B_{max} for AxxA3 at both pH values was significantly lower than WT at both pH values. These results are similar to our previous findings on pH-dependent binding of the focal adhesion protein talin to actin filaments, with pH-insensitive talin mutants having changes in B_{max} but not k_d (17). Moreover, these data suggest that the protonation state of histidines flanked by the Arg/Lys-regions regulates $PI(4,5)P_2$ binding. Consistent with this prediction, the binding of an NHE1 peptide in which the Arg/Lys residues are mutated to alanine (KR/A) had pH-sensitive, but significantly attenuated, $PI(4,5)P_2$-binding (B_{max}, Fig. 2D, Table 1). .

NHE1-RxxR3 and -AxxA3 mutants expressed in fibroblasts have increased and decreased activity, respectively—To determine whether RxxR3 and AxxA3 substitutions affect NHE1 activity, we generated full-length rat NHE1-WT and histidine mutant constructs tagged at the C-terminus with an

HA epitope and stably expressed each construct in NHE1-deficient PS120 fibroblasts that were previously described (8). Immunoblotting cell lysates with HA antibodies showed that NHE1 migrated as a lower molecular weight band corresponding to the immature, core-glycosylated NHE1 and a higher molecular weight band representing the fully processed, highly glycosylated protein (Fig. 3A) (18). We quantified the total NHE1 expression in NHE1-wild type, -AxxA3, and -RxxR3 cells by densitometry (Fig. 3B). Expression of NHE1-AxxA3 was approximately 25% greater than WT and RxxR3 ($p<0.05$), which had similar levels of expression. We also determined surface expression by labeling cells with cell-impermeant biotin and HA-immunoblotting of enriched biotin-modified surface proteins from a streptavidin column. This approach revealed a similar abundance of NHE1-WT, -RxxR3, and -AxxA3 at the cell surface, with the majority of NHE1 at the cell surface corresponding to the highly glycosylated form (Fig. 3C).

Based on B_{max} values for $PI(4,5)P_2$ binding we tested the prediction that NHE1-RxxR3 and NHE1-AxxA3 would have constitutively increased and decreased activity, respectively. We measured time-dependent pHi recoveries from an NH_4Cl-induced acid load in a nominally HCO_3^--free buffer as previously described (8) (Fig. 4A). We also determined NHE1 activity as the pHi-dependent rate of pHi recovery (dpHi/dt) (Fig. 4B,C). For NHE1-WT, quiescent activity increased with platelet-derived growth factor (PDGF; 50 ng/ml), similar to our previous findings (8, 10). At pHi 6.7, quiescent activity of 47.99 ± 5.78 dpHi/dt X 10^{-4} pH/s (mean $\pm$ SD) significantly increased with PDGF to 73.24 ± 9.10 dpHi/dt X 10^{-4} pH/s. For cells expressing NHE1-RxxR3, quiescent activity at pHi 6.7 was 70.34 ± 5.38 dpHi/dt X 10^{-4}

pH/s and significantly greater than quiescent NHE1-WT but not different than NHE1-WT activity with PDGF. Additionally, NHE1-RxxR3 activity did not increase with PDGF, with activity at pH 6.7 of 71.35 ± 6.98 dpHi/dt X 10^{-4} pH/s not significantly different than quiescent. Moreover, quiescent pHi, determined in the presence of 25 mM HCO_3^-, was 7.39 ± 0.04 in cells expressing NHE1-WT and significantly increased with PDGF to 7.56 ± 0.05. Quiescent pHi with RxxR3 was 7.61 ± 0.08, which was significantly higher than with NHE1-WT, and also did not increase with PDGF (Fig. 4D). These data indicate that NHE1-RxxR3 is constitutively more active than NHE1-WT, including generating a higher quiescent pHi.

Activity of NHE1-AxxA3 was significantly lower than NHE1-WT (Fig. 4A-C) and did not increase with PDGF. Activity was 21.43 ± 4.52 dpHi/dt X 10^{-4} pH/s and 25.09 ± 5.15 dpHi/dt X 10^{-4} pH/s in the absence and presence of PDGF, respectively. Notably, NHE1-AxxA3 retained pHi-dependent activity that decreased at higher pHi. Despite the lower activity of NHE1-AxxA3, quiescent pHi in cells expressing this mutant was 7.40 ± 0.06 and not different than that with NHE1-WT. However, pHi with NHE1-AxxA3 did not increase with PDGF (Fig. 4D). Decreased NHE1 activity and, in contrast to our findings, decreased pHi are seen with alanine substitutions in arginine and lysine residues in the charged 513-520 and 556-564 regions with the predicted mechanisms of decreased $PI(4,5)P_2$ binding (13, 15).

In contrast to the lack of response to PDGF, activity of both NHE1-RxxR3 and -AxxA3 increased with hyperosmolarity (Fig. 5A), determined in a nominally HCO_3^--free buffer supplemented with 100 mM NaCl. Compared with their respective quiescent activities indicated above, with hyperosmolarity NHE1-WT activity

increased to 86.25 ± 11.22 dpHi/dt X 10^{-4} pH/s, NHE1-RxxR3 increased to 90.36 ± 9.56 dpHi/dt X 10^{-4} pH/s and NHE1-Axx3 increased to 48.11 ± 2.77 dpHi/dt X 10^{-4} pH/s (Fig. 5B,C). However, hyperosmolarity only increased pHi with expression of NHE1-WT but not NHE1-RxxR3 or NHE1-Axx3 (Fig. 5D). These data suggest that NHE1 activity with hyperosmolarity is mostly independent of PI(4,5)P$_2$ binding, unlike growth factor-regulated activity.

Differences in contractile actin filaments and focal adhesions with NHE1-RxxR3 and -AxxA3—Increased NHE1 activity and pHi promote the assembly of actin filaments (8, 19-21). Consistent with these findings, we observed more contractile actin stress fibers in quiescent cells expressing NHE1-RxxR3 compared with NHE1-WT and -AxxA3 (Fig. 6A). Quantifying the intensity of rhodamine-phalloidin fluorescence confirmed significant differences between the three cell types (Fig. 6B). Additionally, immunolabeling for phosphorylated myosin light chain (pMLC) showed abundant and thick bundled actin filaments traversing the cell length were highly decorated by pMLC with RxxR3. In contrast, actin stress fibers were fewer and appeared thinner and shorter with NHE1-WT and NHE1-AxxA3. With NHE1-WT, pMLC decorated predominantly the distal ends of actin filaments in contrast to the entire length with NHE1-RxxR3. With NHE1-AxxA3, pMLC labeling was mostly punctate with minimal labeling along actin filaments. Of note, actin aggregates, likely Hirano bodies, were seen in all three cell lines and is a feature of the parental PS120 fibroblasts (22).

Increased NHE1 activity and pHi also increase the assembly and maturation of cell-substrate focal adhesions (9, 23). Accordingly, immunolabeling of the focal adhesion-associated protein paxillin showed more and larger peripheral focal adhesions with NHE1-RxxR3 compared with NHE1-WT (Fig. 6C-E). With NHE1-RxxR3 there were pronounced clusters of focal adhesions at cell margins as well as numerous focal contacts along the dorsal cell surface. With NHE1-WT, focal adhesions appeared to be predominantly at cell protrusions, with a limited number of focal contacts at the dorsal cell surface. With NHE1-AxxA3, focal adhesions were similar in size and number to those with NHE1-WT, although punctate paxillin labeling at the dorsal surface was more pronounced. Consistent with differences in focal adhesion abundance, cells were more spread with NHE1-RxxR3 and more fusiform and elongated with NHE1-AxxA3, compared with NHE1-WT. Together, these findings suggest that increased activity with RxxR3 is associated with substantial changes in cell morphology with a contractile phenotype indicated by abundant pMLC-decorated actin stress fibers and focal adhesions.

DISCUSSION

NHE1 is an acid extruder controlling H$^+$ efflux at the plasma membrane and a major regulator of pHi in many cells. For normal pHi homeostasis, NHE1 activity increases in response to acidic pHi and becomes quiescent at neutral pHi. The pHi regulation of NHE1 activity was proposed over 30 years ago to be mediated by an internal H$^+$ modifier site independent of the proton binding site used for substrate transport (11); however, the precise identity of this site remains unclear. Subsequent studies suggested that a proton modifier site located in the C-terminal cytoplasmic domain modulates a set point for NHE1 activity (24, 25) and found that binding PI(4,5)P$_2$ is necessary for maximal NHE1 activity (13, 15), with increased binding at lower pH. However, studies on PI(4,5)P$_2$ binding focused on arginines and lysines in a putative modifier site, which likely do not

change charge within the physiological pH range to regulate binding affinity for anionic phospholipids. We found that a cluster of four histidines in the putative modifier site confer pH-dependent $PI(4,5)P_2$ binding. When these histidines are substituted to arginines, NHE1 has constitutively increased activity and pHi is higher, while alanine substitutions result in significantly decreased activity, although quiescent pHi is not different compared with wild type NHE1. Although RxxR3 and AxxA3 mutants lack pH-dependent $PI(4,5)P_2$ binding and their activity in cells is increased and decreased, respectively, they retain pH sensitivity with greater activity at lower pHi. The pHi-dependent activity of these mutants could be maintained by alternative proton modifier sites that have been proposed in the NHE1 distal C-terminus and transmembrane domain (26).

A pH-dependent "His switch" for binding membrane phospholipids is emerging as a regulatory mechanism for many proteins. However, His switches have predominantly been identified in cytosolic rather than integral membrane proteins. We previously showed that activation of the actin binding protein cofilin at higher pH is mediated by deprotonation of cofilin-His133, which decreases affinity for binding $PI(4,5)P_2$ to release cofilin from its inactive, plasma membrane-bound state (19). We also showed a similar pH-sensitive His switch for releasing membrane-associated Dbs, a guanine nucleotide exchange factor for Cdc42 (27). Additionally, the FYVE domain that targets many proteins, including endosome antigen 1 and guanine nucleotide exchange factors, to intracellular vesicle membranes has two conserved His residues that confer a pH-sensitive His switch for binding phosphatidylinositol 3-phosphate (28, 29). Intracellular membrane targeting of proteins containing ENTH and ANTH domains is also regulated by His switches

for binding membrane phospholipids (30). However, for integral membrane ion transport proteins, the role of pH-dependent His switches for phospholipid binding and activity is less clear. Fliegel and colleagues (31) recognized the histidine cluster in NHE1 we studied, but did not test $PI(4,5)P_2$ binding, and found that human NHE1-[540]HYGAAA and -HYGRRR mutants have no effect on activity, which compared with our results suggests the possibility that His540 may be a critical residue for pH sensing. In the NHE isoform NHE3, His499, which is equivalent to His543 of NHE1 (Fig. 1C), confers pHi sensitive activity (32); however, the role of His499 in $PI(4,5)P_2$ binding was not reported. Additionally, Na-HCO_3 exchangers in the SLC4A family contain multiple histidines within and surrounding a $PI(4,5)P_2$-biding site (33), although to our knowledge the importance of these histidines for $PI(4,5)P_2$ binding has not been reported. Hence, our findings are significant in showing a pH-dependent His switch for $PI(4,5)P_2$ binding that regulates activity of an integral membrane ion transport protein.

Our findings also suggest substantial differences in how growth factors and hyperosmolarity increase NHE1 activity, as activity of NHE1-RxxR3 and -AxxA3 increases with hyperosmolarity but not with PDGF. Hyperosmolarity is proposed to activate NHE1 through a mechanical, cell-shrinkage-dependent mechanism (34) and a predicted volume-sensitive site on NHE1 is different than sites required to mediate the stimulatory effects of growth factors (35). Many growth factors and hormones activate NHE1 by increasing the phosphorylation of distinct serine residues in the distal C terminus of NHE1, with direct phosphorylation confirmed by the kinases p90RSK (7), Akt (8), ROCK (9) and NIK/MAP4K4 (10). Ligand-increased NHE1 activity is inhibited by alanine

substitutions in these serine residues. However, activity of the NHE1-AxxA3 mutant is significantly lower compared with wild type and does not increase with PDGF, which suggests that for wild type NHE1, PI(4,5)P$_2$ binding by the membrane-proximal C-terminus and phosphorylation of the distal C-terminus are integrated. If the set point or pH-dependence of a proton modifier site is changed by ligand-dependent NHE1 phosphorylation, it remains to be determined whether the pK$_a$ values of histidine residues regulating PI(4,5)P$_2$ binding might be upshifted. Wakabayshi and colleagues proposed that growth factors and hormones increasing diacylglycerol activate NHE1 through a lipid-interacting domain (LID) encompassing amino acids 542–598 in human NHE1 that includes the PI(4,5)P$_2$ binding region (36, 37). They found that the LID domain binds phorbol esters and used FRET reporters to show increased association of the NHE1 C-terminus with the plasma membrane in cell treated with phorbol esters. However, phorbol ester and PI(4,5)P$_2$ binding within the LID may be distinct because alanine substitutions for Leu-573 and Ile-574 were identified as mediators of phorbol ester binding (36). Recent work from Schelling and colleagues suggests that decreased NHE1 activity from disrupted PI(4,5)P$_2$ binding contributes to apoptosis in renal tubular atrophy (38). They found that amphipathic, long chain acyl-CoA metabolites, which accumulate with glomerular injury, decrease NHE1 activity by competing with PI(4,5)P$_2$ binding. Future studies could address whether a similar competitive inhibition of PI(4,5)P$_2$ binding might contribute to the proposed NHE1-dependent apoptosis in neurodegenerative diseases (5).

Although we currently lack a unified mechanistic description for the complex interplay of regulated NHE1 activity, many publications described here indicate the importance of PI(4,5)P$_2$ binding. Our findings reveal the critical significance of a histidine cluster for PI(4,5)P$_2$ binding, which contributes to the established pHi-dependence of NHE1 activity. Beyond insights on mechanisms regulating NHE1 activity, the constitutively active NHE1-RxxR3 mutant we report has promise as a new tool for determining functional consequences of increased pHi, particularly in cancer cell biology, based on increased pHi with activated oncogene and our recent finding (4) that increased pHi in the absence of activated oncogenes is sufficient to induce hyperproliferation and dysplasia.

EXPERIMENTAL PROCEDURES
Sequence Alignment of NHE1 C-terminal Juxtamembrane Region—The sequence surrounding the His-rich region of human NHE1 was aligned to NHE1 orthologs from other species and to other human plasma membrane NHE family members (NHE2-5) using Clustal Omega (39). NCBI Accession numbers used for alignment: *Homo sapiens* NHE1 – NP_003038.2; *Homo sapiens* NHE2 – NP_003039.2; *Homo sapiens* NHE3 – NP_004165.2; *Homo sapiens* NHE4 – NP_001011552.2; *Homo sapiens* NHE5 – NP_004585.1; *Mus musculus* NHE1 – NP_058677.1; *Rattus norvegicus* NHE1 – NP_036784.1; *Gallus gallus* NHE1 – NP_001038108.1; *Xenopus laevis* NHE1 – NP_001081553.1; *Danio rerio* NHE1 – NP_001106952.1.

Expression and Purification of GST-NHE1 503-815—The C-terminal cytoplasmic domain of human NHE1 (amino acids 503-815) in the pGEX vector was previously described (10). Site directed mutagenesis was used to mutate His540, 543, 544, and 545 to alanines or arginines (QuikChange Lightning, Agilent, Santa Clara, CA). DNA primers were designed using an online

primer design tool (http://www.genomics.agilent.com/primerDesignProgram.jsp) and purchased from Elim Biopharmaceuticals (Hayward, CA). DNA sequencing was performed to verify mutations. Expression and affinity purification of wild type and mutant GST-NHE1 was performed as previously described (22). Protein was concentrated using an Amicon Ultracel-20K Centrifugal Filter Unit and stored at 4°C. Protein integrity and purity were determined by Coomassie blue stained SDS-PAGE gels.

ELISA PI(4,5)P₂-binding Assay—Pre-blocked Cova PI(4,5)P₂ screening plates (Echelon Biosciences, Salt Lake City, UT, catalog number 1278H-6) were used for binding assays. Wild type and mutant GST-NHE1 were incubated at concentrations from 0-1 μM in binding buffer (10 mM HEPES, 150 mM NaCl, 1% mouse serum) of pH 7.5 or 7.0 for one hour at room temperature. Wells were washed three times (3 minutes each) with wash buffer (binding buffer + 0.05% Tween-20) and incubated for one hour at room temperature with peroxidase-conjugated anti-GST antibody (Abcam, Cambridge, MA, catalog number ab137840, lot number GR169731-2) diluted 1:5,000 in binding buffer. After washing three times, 100 μl of 3,3',5,5'-tetramethylbenzidine (Sigma Aldrich, catalog number T8665, lot number SLBM6117V) was added to each well for 15 minutes and the optical density read at 370 nm on a SpectraMax M5 plate reader (Molecular Dynamics, Sunnyvale, CA). Statistical analyses were performed using GraphPad software.

Cell Expression of Recombinant NHE1— The mammalian expression construct, pCMV-NHE1, containing the full-length rat NHE1 sequence and a 3' HA epitope tag was previously described (22, 40, 41). Site

directed mutagenesis was used to mutate His544, 547, 548, and 549 to alanines or arginines as described above. Wild type and mutant NHE1-HA were stably expressed in NHE1-deficient PS120 cells, derived from CCL39 hamster lung fibroblasts as described (22). Cells were maintained in Dubecco's modified Eagle medium (DMEM) supplemented with 5% FBS and penicillin/streptomycin (complete media). The expression of wild type and mutant NHE1 was determined by immunoblotting of cell lysates while the cell surface expression was determined by the selective biotinylation and isolation of cell surface proteins using a commercially available kit (Pierce Cell Surface Protein Isolation Kit, ThermoFisher Scientific, catalog number 89881). Proteins were separated by SDS-PAGE and transferred to polyvinylidene difluoride membranes for immunoblotting. The membranes were probed with mouse anti-HA (12CA5) epitope tag (1:1000, ThermoFisher Scientific, catalog number MA1-12429) for NHE1-HA or mouse anti-actin clone C4 (1:5,000, ED Millipore MAB1501) as a loading control. Peroxidase-conjugated goat anti-mouse (BioRad Laboratories, catalog number 172-6516, lot number 350003069) and goat anti-rabbit secondary antibodies (BioRad Laboratories, catalog number 172-1019, lot number 350003011) were used at a 1:10,000 dilution. Bound antibodies were detected by enhanced chemiluminescence.

NHE1 Activity—NHE1 activity was determined as the rate of pHi recovery (dpHi/dt) from an NH₄Cl-induced acid load, as previously described (8). Briefly, cells were plated in triplicate for each condition and maintained in complete medium for 24 h before incubating with DMEM containing 0.2% FBS for 20 h to induce quiescence. Cells loaded with 1 μM 2,7-biscarboxyethyl-5(6)-carboxyfluorescein

(BCECF; Invitrogen) in a nominally HCO_3^--free HEPES buffer were incubated for 10 min in HEPES buffer containing 40 mM NH_4Cl, which was rapidly aspirated and replaced with HEPES buffer in the absence (control) or presence of PDGF (50 ng/ml) or NaCl (100 mM). Ratios of BCECF fluorescence at Ex490/Em530 and Ex440/Em530 were acquired every 15 seconds for 5 minutes. Fluorescence ratios were converted to pHi by calibrating each well with 10 µM nigericin (Invitrogen) at pH 7.4 and pH 6.6. NHE1 activity was expressed as dpHi/dt by evaluating the derivative of the slope of the time-dependent pHi recovery at intervals of 0.05 pH units and statistical analyses were performed using GraphPad software. Steady-state pHi was determined as previously described (8). In brief, quiescent cells loaded with BCECF in buffer containing 25 mM HCO_3^- were washed and incubated in HCO_3^- buffer in the absence or presence of PDGF or NaCl for 5 min before measuring fluorescence ratios and calibrating pHi as described above.

Immunolabeling—Immunocytochemistry was performed as previously described (8). In brief cells plated at a density of 50 X 10^4 cells/well of a 6-well plate containing 100 mm glass coverslips were maintained in complete medium for 24 h, washed and maintained in DMEM containing 0.2% FBS for 20 hours. After washing with 100 mM phosphate buffer (PB), cells were fixed in 4% paraformaldehyde in PB for 10 min, permeabilized in 0.1% Triton X-100 in PB for 10 min and incubated in blocking PB containing 2% FBS for 60 min. Cells were incubated overnight at 4°C with primary antibodies to phosphoMLC (T18/S19, rabbit, Cell Signaling Technologies, catalog number 3674, lot number 5) and paxillin (mouse, BD Transduction Laboratories,

catalog number 610620, lot number 66614) diluted 1:200 in PB containing 0.01% Triton X-100. After washing with PB cells were incubated for 1 h with PB containing secondary antibodies Alexa Fluor 488 goat anti-rabbit (ThermoFisher Scientific, catalog number A11008, lot number 458548) or goat anti-mouse (ThermoFisher Scientific, catalog number A11001, lot number 455497) (1:200) and rhodamine-phalloidin (ThermoFisher Scientific, catalog number R415, lot number 1616945) (1:400). Fluorescence images were acquired using a spinning disk confocal (Yokogawa; CSU-10) on a microscope (Nikon; TE-2000) with a 60X objective (Plan TIRF 1.49 NA) equipped with a cooled CCD camera and analyzed using NIS-Elements software (Nikon). To quantify rhodamine-phalloidin fluorescence, background subtraction was first performed from an ROI that did not include cells and then mean background-subtracted rhodamine fluorescence was determined as the average of three uniform regions of interest for each of the indicated number of cells in three separate preparations. Quantitative analysis of focal adhesions was performed on maximum intensity projections generated from a z-stack. Background subtraction was performed from an ROI that did not include cells. Focal adhesions were selected for analysis if they were located near or touching plasma membrane and had actin filaments terminating within. The "Auto detect ROI" tool with a GUI tuning parameters setting of 5 was used to select ROIs. Area and mean intensity of each focal adhesion was quantified and exported to Microsoft Excel for analysis; graphs were generated using Prism. Outliers greater than two standard deviations from the mean were excluded from the final analysis.

Conflict of Interest

The authors declare no competing financial interests.

Author Contributions
BAW and AS conceived initial studies. BAW generated and characterized NHE1 expression in cell lines, including surface biotinylation and abundance, and acquired images for focal adhesion immunolabeling.. KAW performed and analyzed *in vitro* PI(4,5)P$_2$ binding assays. BKGH performed quantification of focal adhesions. AS generated GST constructs used in *in vitro* binding assays and performed initial characterization of lipid binding. CC performed western blot analysis. DLB performed NHE1 activity assays, pHi determinations, labeling and imaging of actin filaments and pMLC, as well as quantification of actin filaments. BAW, KAW, BKGH and DLB contributed to the writing of this manuscript.

References
1. Boron, W. (2004) Regulation of intracellular pH. *Advances in physiology education*. **28**, 160

2. Cardone, R. A., Casavola, V., and Reshkin, S. J. (2005) The role of disturbed pH dynamics and the Na+/H+ exchanger in metastasis. *Nat Rev Cancer*. **5**, 786–795

3. Webb, B. A., Chimenti, M., Jacobson, M. P., and Barber, D. L. (2011) Dysregulated pH: a perfect storm for cancer progression. *Nat Rev Cancer*. **11**, 671–677

4. Grillo-Hill, B. K., Choi, C., Jimenez-Vidal, M., and Barber, D. L. (2015) Increased H$^+$ efflux is sufficient to induce dysplasia and necessary for viability with oncogene expression. *eLife*. 10.7554/eLife.03270

5. Harguindey, S., Reshkin, S. J., Orive, G., Arranz, J. L., and Anitua, E. (2007) Growth and trophic factors, pH and the Na+/H+ exchanger in Alzheimer's disease, other neurodegenerative diseases and cancer: new therapeutic possibilities and potential dangers. *Curr Alzheimer Res*. **4**, 53–65

6. Fang, B., Wang, D., Huang, M., Yu, G., and Li, H. (2010) Hypothesis on the relationship between the change in intracellular pH and incidence of sporadic Alzheimer's disease or vascular dementia. *Int. J. Neurosci.* **120**, 591–595

7. Takahashi, E., Abe, J., Gallis, B., Aebersold, R., Spring, D. J., Krebs, E. G., and Berk, B. C. (1999) p90(RSK) is a serum-stimulated Na+/H+ exchanger isoform-1 kinase. Regulatory phosphorylation of serine 703 of Na+/H+ exchanger isoform-1. *J Biol Chem*. **274**, 20206–20214

8. Meima, M. E., Webb, B. A., Witkowska, H. E., and Barber, D. L. (2009) The sodium-hydrogen exchanger NHE1 is an Akt substrate necessary for actin filament reorganization by growth factors. *J Biol Chem*. **284**, 26666–26675

9. Tominaga, T., Ishizaki, T., Narumiya, S., and Barber, D. L. (1998) p160ROCK mediates RhoA activation of Na-H exchange. *EMBO J*. **17**, 4712–4722

10. Yan, W., Nehrke, K., Choi, J., and Barber, D. L. (2001) The Nck-interacting kinase (NIK) phosphorylates the Na+-H+ exchanger NHE1 and regulates NHE1 activation by platelet-derived growth factor. *J Biol Chem*. **276**, 31349–31356

11. Aronson, P. S., Nee, J., and Suhm, M. A. (1982) Modifier role of internal H+ in activating the Na+–H+ exchanger in renal microvillus membrane vesicles. *Nature*. **299**, 161–163

12. Hilgemann, D. W., Feng, S., and Nasuhoglu, C. (2001) The complex and intriguing lives of PIP2 with ion channels and transporters. *Sci. STKE*. **2001**, re19

13. Aharonovitz, O., Zaun, H. C., Balla, T., York, J. D., Orlowski, J., and Grinstein, S. (2000)

Intracellular pH regulation by Na(+)/H(+) exchange requires phosphatidylinositol 4,5-bisphosphate. *J Cell Biol*. **150**, 213–224

14. Alexander, R. T., Jaumouillé, V., Yeung, T., Furuya, W., Peltekova, I., Boucher, A., Zasloff, M., Orlowski, J., and Grinstein, S. (2011) Membrane surface charge dictates the structure and function of the epithelial Na+/H+ exchanger. *EMBO J*. **30**, 679–691

15. Abu Jawdeh, B. G., Khan, S., Deschênes, I., Hoshi, M., Goel, M., Lock, J. T., Shinlapawittayatorn, K., Babcock, G., Lakhe-Reddy, S., DeCaro, G., Yadav, S. P., Mohan, M. L., Naga Prasad, S. V., Schilling, W. P., Ficker, E., and Schelling, J. R. (2011) Phosphoinositide binding differentially regulates NHE1 Na+/H+ exchanger-dependent proximal tubule cell survival. *J Biol Chem*. **286**, 42435–42445

16. Schönichen, A., Webb, B. A., Jacobson, M. P., and Barber, D. L. (2013) Considering protonation as a posttranslational modification regulating protein structure and function. *Annu Rev Biophys*. **42**, 289–314

17. Srivastava, J., Barreiro, G., Groscurth, S., Gingras, A. R., Goult, B. T., Critchley, D. R., Kelly, M. J. S., Jacobson, M. P., and Barber, D. L. (2008) Structural model and functional significance of pH-dependent talin-actin binding for focal adhesion remodeling. *Proc Natl Acad Sci USA*. **105**, 14436–14441

18. Counillon, L., Pouyssegur, J., and Reithmeier, R. A. (1994) The Na+/H+ exchanger NHE-1 possesses N- and O-linked glycosylation restricted to the first N-terminal extracellular domain. *Biochemistry*. **33**, 10463–10469

19. Frantz, C., Barreiro, G., Dominguez, L., Chen, X., Eddy, R., Condeelis, J., Kelly, M. J. S., Jacobson, M. P., and Barber, D. L. (2008) Cofilin is a pH sensor for actin free barbed end formation: role of phosphoinositide binding. *J Cell Biol.* **183**, 865–879

20. Magalhaes, M. A. O., Larson, D. R., Mader, C. C., Bravo-Cordero, J. J., Gil-Henn, H., Oser, M., Chen, X., Koleske, A. J., and Condeelis, J. (2011) Cortactin phosphorylation regulates cell invasion through a pH-dependent pathway. *J Cell Biol*. **195**, 903–920

21. Clement, D. L., Mally, S., Stock, C., Lethan, M., Satir, P., Schwab, A., Pedersen, S. F., and Christensen, S. T. (2013) PDGFRα signaling in the primary cilium regulates NHE1-dependent fibroblast migration via coordinated differential activity of MEK1/2-ERK1/2-p90RSK and AKT signaling pathways. *J Cell Sci*. **126**, 953–965

22. Denker, S. P., Huang, D. C., Orlowski, J., Furthmayr, H., and Barber, D. L. (2000) Direct binding of the Na--H exchanger NHE1 to ERM proteins regulates the cortical cytoskeleton and cell shape independently of H(+) translocation. *Mol Cell*. **6**, 1425–1436

23. Choi, C.-H., Webb, B. A., Chimenti, M. S., Jacobson, M. P., and Barber, D. L. (2013) pH sensing by FAK-His58 regulates focal adhesion remodeling. *J Cell Biol*. **202**, 849–859

24. Wakabayashi, S., Bertrand, B., Shigekawa, M., Fafournoux, P., and Pouyssegur, J. (1994) Growth factor activation and "H(+)-sensing" of the Na+/H+ exchanger isoform 1 (NHE1). Evidence for an additional mechanism not requiring direct phosphorylation. *J Biol Chem*. **269**, 5583–5588

25. Orlowski, J., and Grinstein, S. (1997) Na+/H+ exchangers of mammalian cells. *J Biol Chem*. **272**, 22373–22376

26. Wakabayashi, S., Ikeda, T., Iwamoto, T., Pouyssegur, J., and Shigekawa, M. (1997) Calmodulin-binding autoinhibitory domain controls "pH-sensing" in the Na+/H+ exchanger NHE1 through sequence-specific interaction. *Biochemistry*. **36**, 12854–12861

27. Frantz, C., Karydis, A., Nalbant, P., Hahn, K. M., and Barber, D. L. (2007) Positive feedback between Cdc42 activity and H+ efflux by the Na-H exchanger NHE1 for polarity

of migrating cells. *J Cell Biol*. **179**, 403–410

28. Lee, S. A., Eyeson, R., Cheever, M. L., Geng, J., Verkhusha, V. V., Burd, C., Overduin, M., and Kutateladze, T. G. (2005) Targeting of the FYVE domain to endosomal membranes is regulated by a histidine switch. *Proc Natl Acad Sci USA*. **102**, 13052–13057

29. He, J., Vora, M., Haney, R. M., Filonov, G. S., Musselman, C. A., Burd, C. G., Kutateladze, A. G., Verkhusha, V. V., Stahelin, R. V., and Kutateladze, T. G. (2009) Membrane insertion of the FYVE domain is modulated by pH. *Proteins*. **76**, 852–860

30. Hom, R. A., Vora, M., Regner, M., Subach, O. M., Cho, W., Verkhusha, V. V., Stahelin, R. V., and Kutateladze, T. G. (2007) pH-dependent binding of the Epsin ENTH domain and the AP180 ANTH domain to PI(4,5)P2-containing bilayers. *J Mol Biol.* **373**, 412–423

31. Dibrov, P., Murtazina, R., Kinsella, J., and Fliegel, L. (2000) Characterization of a histidine rich cluster of amino acids in the cytoplasmic domain of the Na+/H+ exchanger. *Biosci. Rep.* **20**, 185–197

32. Cha, B., Oh, S., Shanmugaratnam, J., Donowitz, M., and Yun, C. C. (2003) Two histidine residues in the juxta-membrane cytoplasmic domain of Na+/H+ exchanger isoform 3 (NHE3) determine the set point. *J. Membr. Biol.* **191**, 49–58

33. Hong, J. H., Yang, D., Shcheynikov, N., Ohana, E., Shin, D. M., and Muallem, S. (2013) Convergence of IRBIT, phosphatidylinositol (4,5) bisphosphate, and WNK/SPAK kinases in regulation of the Na+-HCO3- cotransporters family. *Proc Natl Acad Sci USA.* **110**, 4105–4110

34. Krump, E., Nikitas, K., and Grinstein, S. (1997) Induction of tyrosine phosphorylation and Na+/H+ exchanger activation during shrinkage of human neutrophils. *J Biol Chem*. **272**, 17303–17311

35. Bianchini, L., Kapus, A., Lukacs, G., Wasan, S., Wakabayashi, S., Pouyssegur, J., Yu, F. H., Orlowski, J., and Grinstein, S. (1995) Responsiveness of mutants of NHE1 isoform of Na+/H+ antiport to osmotic stress. *Am J Physiol*. **269**, C998–1007

36. Wakabayashi, S., Nakamura, T. Y., Kobayashi, S., and Hisamitsu, T. (2010) Novel Phorbol Ester-binding Motif Mediates Hormonal Activation of Na+/H+ Exchanger. *J Biol Chem*. **285**, 26652–26661

37. Shimada-Shimizu, N., Hisamitsu, T., Nakamura, T. Y., Hirayama, N., and Wakabayashi, S. (2014) Na+/H+ exchanger 1 is regulated via its lipid-interacting domain, which functions as a molecular switch: a pharmacological approach using indolocarbazole compounds. *Mol Pharmacol*. **85**, 18–28

38. Khan, S., Abu Jawdeh, B. G., Goel, M., Schilling, W. P., Parker, M. D., Puchowicz, M. A., Yadav, S. P., Harris, R. C., El-Meanawy, A., Hoshi, M., Shinlapawittayatorn, K., Deschênes, I., Ficker, E., and Schelling, J. R. (2014) Lipotoxic disruption of NHE1 interaction with PI(4,5)P2 expedites proximal tubule apoptosis. *J Clin Invest*. **124**, 1057–1068

39. Sievers, F., Wilm, A., Dineen, D., Gibson, T. J., Karplus, K., Li, W., Lopez, R., McWilliam, H., Remmert, M., Söding, J., Thompson, J. D., and Higgins, D. G. (2011) Fast, scalable generation of high-quality protein multiple sequence alignments using Clustal Omega. *Mol. Syst. Biol.* **7**, 539

40. Kapus, A., Grinstein, S., Wasan, S., Kandasamy, R., and Orlowski, J. (1994) Functional characterization of three isoforms of the Na+/H+ exchanger stably expressed in Chinese hamster ovary cells. ATP dependence, osmotic sensitivity, and role in cell proliferation. *J Biol Chem*. **269**, 23544–23552

41. Orlowski, J. (1993) Heterologous expression and functional properties of amiloride high affinity (NHE-1) and low affinity (NHE-3) isoforms of the rat Na/H exchanger. *J Biol Chem*. **268**, 16369–16377

FOOTNOTES

The abbreviations used are: NHE1, sodium hydrogen exchanger 1; PI(4,5)P$_2$, phosphatidylinositol 4,5-bisphosphate; pHi, intracellular pH.

FIGURE LEGENDS

FIGURE 1. A cluster of histidine residues in the PI(4,5)P$_2$-binding domain of NHE1 is evolutionarily conserved. A) Schematic diagram of NHE1 and the location of the two lysine/arginine-rich PI(4,5)P$_2$ binding site (K/R1, K/R2) surrounding a poly-histidine region (HxxHHH). B) Sequence alignment of NHE1 orthologs. The His-rich region is shown in red. C) Sequence alignment of membrane binding regions of plasma membrane NHE's. Blue, phospholipid binding region KR1. Green, phospholipid binding region KR2. Red, histidine cluster located between KR1 and KR2. NCBI Accession numbers for sequences: NHE1 – NP_003038.2; NHE2 – NP_003039.2; NHE3 – NP_004165.2; NHE4 – NP_001011552.2; NHE5 – NP_004585.1.

FIGURE 2. A cluster of histidine residues mediate pH-dependent PI(4,5)P$_2$ binding by NHE1. A-D) PI(4,5)P$_2$ binding at pH 7.0 (dotted line) and pH 7.5 (solid line) for wild type (A, black), RxxR3 (B, red), and AxxA3 (C, blue) and KR/A (D, orange). D' shows the same data in D with a magnified y-axis. Data are mean ± SD from 6 experiments for A-C and 3 experiments for D. E) Coomassie-stained SDS-PAGE of wild type (WT), RxxR3 (R), AxxA3 (A), and KR/A GST-NHE1 503-815 proteins. The size of the molecular weight marker (MW) is shown in kDa.
.

FIGURE 3. Expression of NHE1-WT and histidine mutants in fibroblasts. A) HA and actin immunoblots of total lysates from NHE1-deficient PS120 cells and cells stably expressing NHE1-wild type (WT), -RxxR3 and -AxxA3 tagged with an HA epitope. B) Relative NHE1 expression in AxxA3 and RxxR3 cells was quantified from Western blots by densitometry. The total NHE1 signal, representing the immature and processed forms of NHE1, was normalized to actin and expressed as a fold wild type. Bars represent the mean ± SD and grey dots represent relative NHE/actin ratio from 5 independent preparations of cells. *, P<0.05. C) HA immunoblot

of enriched biotinylated cell surface proteins. Data are representative of experiments from two separate cell preparations. The molecular weight marker (MW) is shown in kDa.

FIGURE 4. Histidine mutants have distinct quiescent activities that do not increase with PDGF. NHE1 activity was determined as the rate of pHi recovery from an NH_4Cl-induced acid load in cells loaded with the pH-sensitive dye BCECF. A) Means of time-dependent pHi recoveries in the absence (quiescent; solid lines) and presence of PDGF (50 ng/ml; dotted lines) from five independent cell preparations. B) Means of pHi-dependent recovery rates (dpHi/dt) in the absence (quiescent; solid lines) and presence of PDGF (50 ng/ml; dotted lines) from six independent cell preparations. C) dpHi/dt at pHi 6.6 in quiescent and PDGF-treated cells from data shown in (C). Data are means ± SD of six independent cell preparations. D) The pHi of indicated cell types at quiescence and with PDGF (50 ng/ml PDGF for 5 min). Data are means ± SD of six independent cell preparations. *** p<0.001

FIGURE 5. Histidine mutants retain increased activity with hyperosmolarity. A) Means of time-dependent pHi recoveries in the absence (quiescent; solid line) and presence of excess 100 mM NaCl (dotted lines) from four independent cell preparations. B) Means of pHi-dependent recoveries (dpHi/dt) in the absence (quiescent; solid lines) and presence of excess 100 mM NaCl (dotted lines) from four independent cell preparations. C) dpHi/dt) at pHi 6.6 for data shown in (C). Data are means ± SD of six independent cell preparations. D) The pHi of indicated cell types at quiescence and with 100 mM NaCl (5 min). Data are means ± SD of six independent cell preparations. ** p< 0.01; *** p<0.001

FIGURE 6. Histidine mutants have differences in abundance of contractile actin filaments and focal adhesions. **A)** Representative confocal images of the indicated cell types at quiescence labeled with pMLC (green) and rhodamine-phalloidin (magenta). B) Mean fluorescence intensities of rhodamine-phalloidin for WT (53 cells), RxxR3 (42 cells), and AxxA3 (58 cells) in three separate cell preparations. (C) Representative confocal images of the indicated cell types at quiescence labeled with paxillin (green) and rhodamine phalloidin (magenta). Paxillin labeling is also shown in monochromatic LUT. D,E) Quantification of the peripheral focal adhesion number per cell (D) and area per cell (E). WT (43 cells), RxxR3 (41 cells), and AxxA3 (49 cells) in three independent cell preparations. ** p<0.01, *** p<0.001.

TABLE 1 - Binding parameters from ELISA PI(4,5)P2 experiments. The maximal binding, B_{max}, is reported in arbitrary units (a.u.). The dissociation constant, k_d, is reported in nM. Data are mean ± SD from 3 (KR/A) and 6 (WT, AxxA3, RxxR3) independent experiments. *, p<0.05 compared to pH 7.5. &, p<0.001 compared to pH 7.5. $, p<0.05 compared to WT and RxxR3 at pH 7.0. #, p<0.05 compared to WT and RxxR3 at pH 7.5. @, p<0.01 compared to WT. n.d., not determined.

Construct	B_{max}		k_d	
	pH 7.5	pH 7.0	pH 7.5	pH 7.0
wild type	0.87 ± 0.04	1.00 ± 0.04*	65 ± 10	38 ± 6*
AxxA3	0.76 ± 0.04 [#]	0.79 ± 0.03 [$]	78 ± 14	62 ± 9 [$]
RxxR3	0.97 ± 0.05	0.97 ± 0.03	67 ± 13	44 ± 5
KR/A	0.16 ± 0.04 [@]	0.27 ± 0.01 [&,@]	n.d.	n.d.

A

NHE1

KR1   KR2

HxxHHH
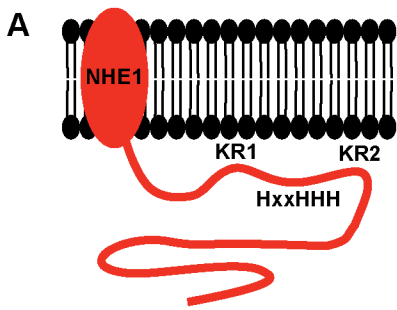
B

Homo sapiens	534	IEDICG**H**YG**HHH**WKDKLN	551
Mus musculus	538	IEDICG**H**YG**HHH**WKDKLN	555
Rattus norvegicus	538	IEDICG**H**YG**HHH**WKDKLN	555
Gallus gallus	526	IEDICG**H**YG**HHH**WKDKLN	543
Xenopus laevis	514	IEDICG**H**YG**HHH**WKDKLN	531
Danio rerio	474	IEDVCG**H**YG**HHH**WRDKLS	491

:******:***.

C

NHE1 509 **KKK**QET**KR**SINEEIHTQFLDHLLTGIEDICG**H**YG**HHH**WKDKLN**RFN**KK**YVKK** 560
NHE2 489 **KR**SN**KK**QQAVSEEIYCRLFDHVKTGIEDVCG**H**WG**H**NFWRDKFK**K**FDD**KYL**RK** 540
NHE3 466 **KR**SEH**R**EP**R**LNEKLHGRAFDHILSAIEDISGQIG**H**NYLRDKWSHFD**RK**FLS**R** 517
NHE4 481 V**KK**TN**KK**ESINEELHIRLMDHLKAGIEDVCG**H**WS**H**YQVRDKFK**K**FDH**RYL**RK** 532
NHE5 459 **KR**SEHH**K**PTLNQELHEHTFDHILAAVEDVVG**HH**GY**H**YWRDRWEQFD**KK**YLSQ 510

:. . : :.:::: : :**: :.:**: *: .: :*: .:*: ::: :

Webb et al., Fig. 1

A

Whole Cell   Lysate

MW   PS120   WT   AxxA3   RxxR3

IB: HA

100

75

50

IB: actin

37

B

*

2.0

1.5

1.0

0.5

0.0

Fold WT (NHE1/actin)

AxxA3   RxxR3
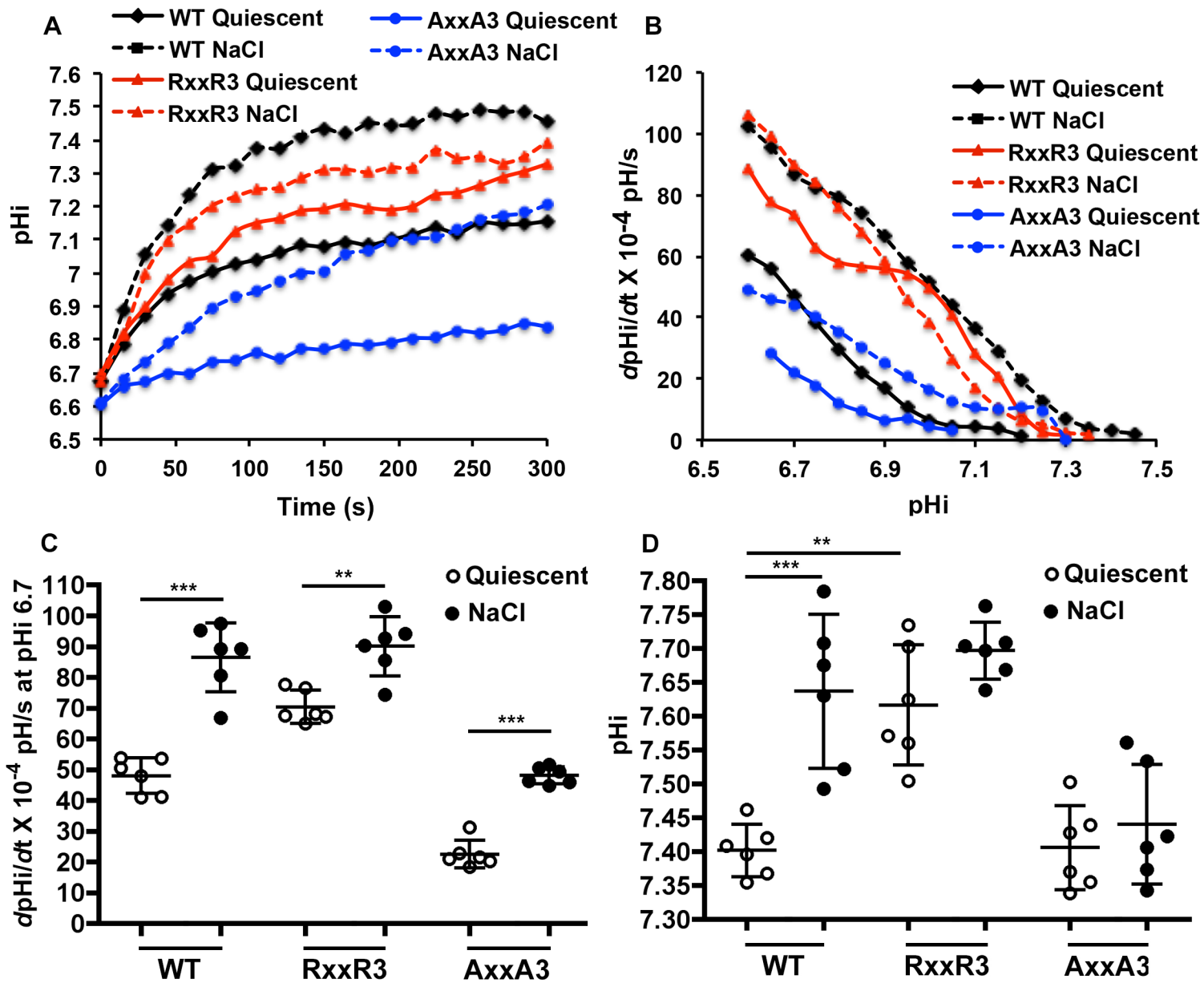
C

Surface   Biotinylation

MW   PS120   WT   AxxA3   RxxR3

IB: HA

100

75
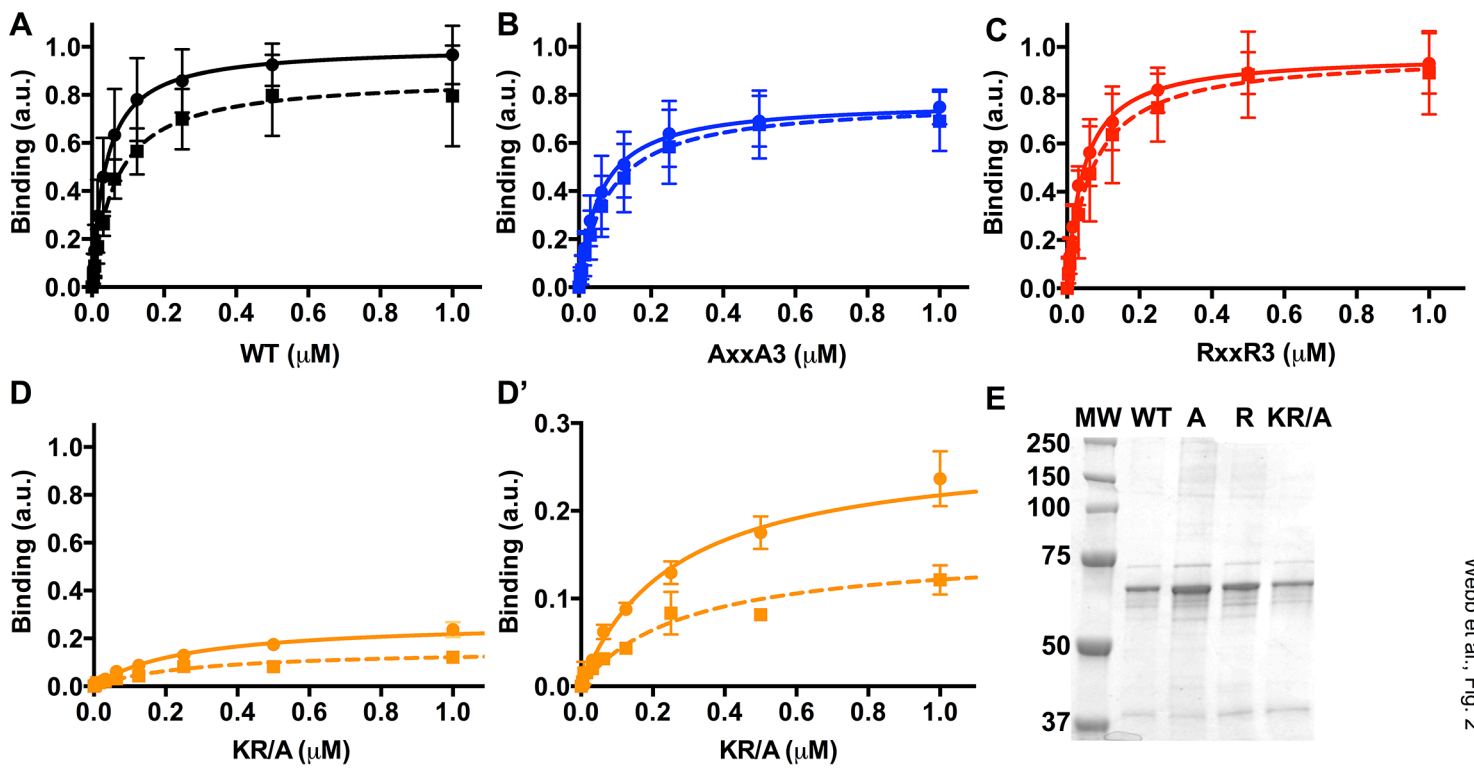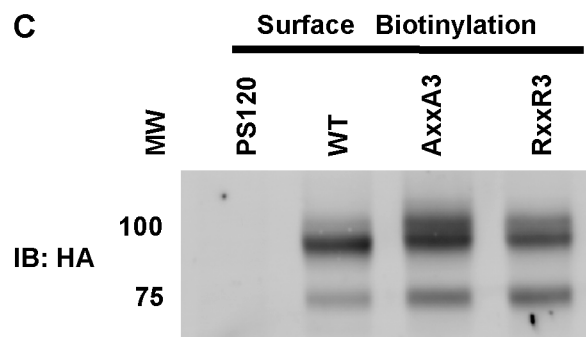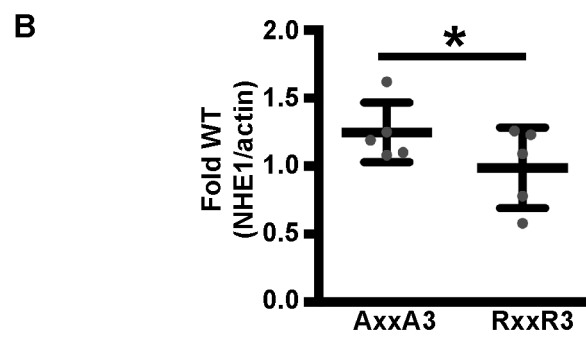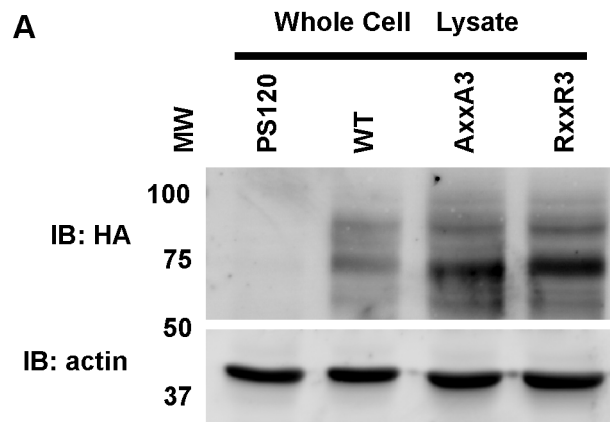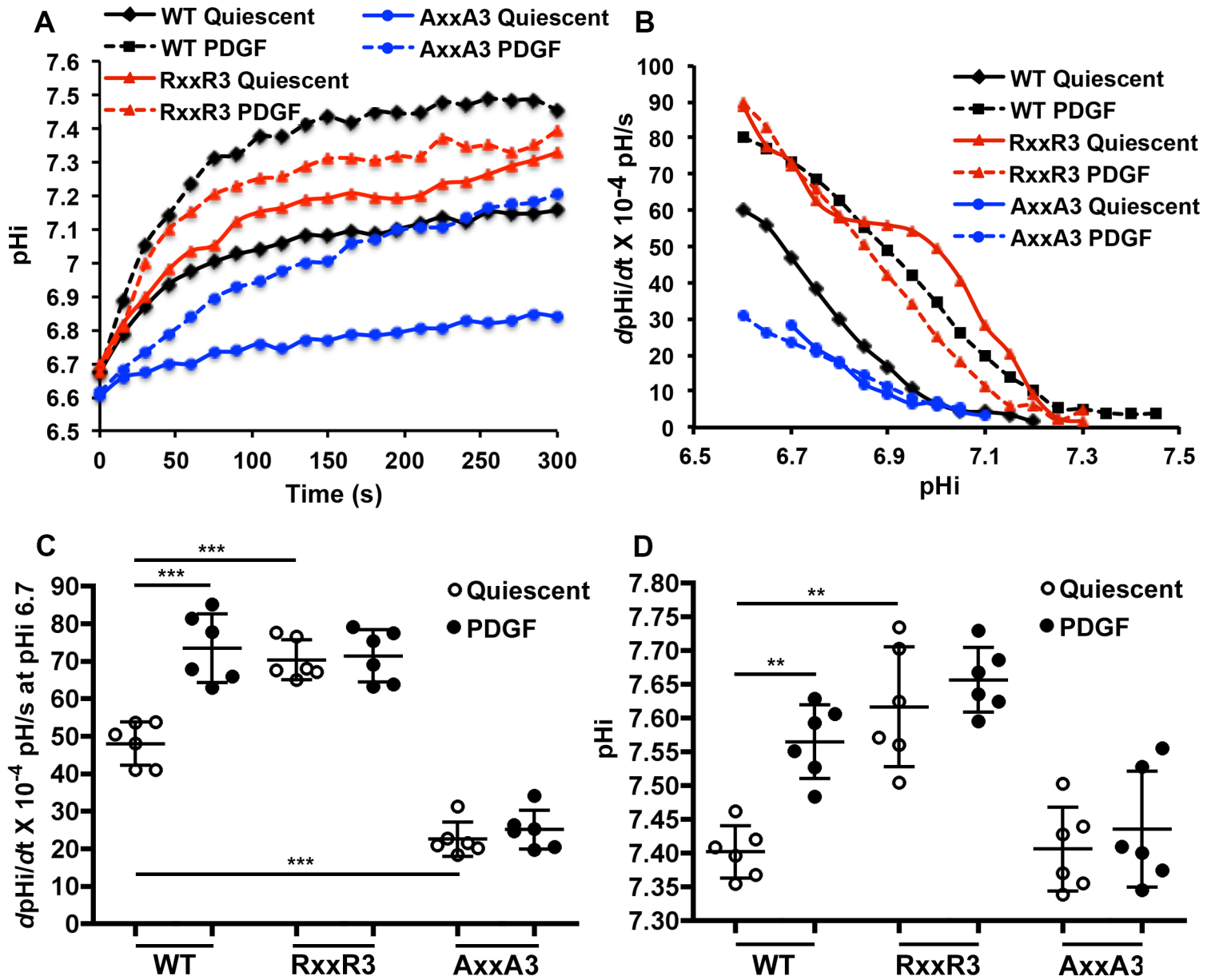
Webb et al., Fig. 4

Webb et al., Fig. 5

A

	pMLC	Phalloidin	Overlay
WT			
RxxR3			
AxxA3			

20 μm

B

Phalloidin Mean Intensity (arbitrary units X10³)

***
***

WT   RxxR3   AxxA3

C

	Paxillin	Overlay
WT		
RxxR3		
AxxA3		

20 μm

D

Focal Adhesion Area per cell (μm²)

**

WT   RxxR3   AxxA3

E

Focal Adhesions per cell

**

WT   RxxR3   AxxA3

Webb et.al., Fig. 6